



UNIVERSITY OF LEEDS

This is a repository copy of *Targeting KNa1.1 channels in KCNT1-associated epilepsy*.

White Rose Research Online URL for this paper:

<https://eprints.whiterose.ac.uk/174791/>

Version: Accepted Version

Article:

Cole, BA, Clapcote, SJ, Muench, SP et al. (1 more author) (2021) Targeting KNa1.1 channels in KCNT1-associated epilepsy. *Trends in Pharmacological Sciences*. ISSN 0165-6147

<https://doi.org/10.1016/j.tips.2021.05.003>

© 2021, Elsevier. This manuscript version is made available under the CC-BY-NC-ND 4.0 license <http://creativecommons.org/licenses/by-nc-nd/4.0/>.

Reuse

This article is distributed under the terms of the Creative Commons Attribution-NonCommercial-NoDerivs (CC BY-NC-ND) licence. This licence only allows you to download this work and share it with others as long as you credit the authors, but you can't change the article in any way or use it commercially. More information and the full terms of the licence here: <https://creativecommons.org/licenses/>

Takedown

If you consider content in White Rose Research Online to be in breach of UK law, please notify us by emailing eprints@whiterose.ac.uk including the URL of the record and the reason for the withdrawal request.



eprints@whiterose.ac.uk
<https://eprints.whiterose.ac.uk/>

1 **Targeting K_{Na}1.1 channels in *KCNT1*-associated epilepsy**

2

3 Bethan A. Cole, Steven J. Clapcote, Stephen P. Muench, and Jonathan D. Lippiat*

4 School of Biomedical Sciences, University of Leeds, Leeds, LS2 9JT, UK

5

6 *Correspondence: j.d.lippiat@leeds.ac.uk

7

8 **Keywords:** Epilepsy, EIMFS, (AD)SHE, KCNT1, K_{Na}1.1, potassium channel

9

10 **Abstract**

11

12 Gain-of-function (GOF) pathogenic variants of *KCNT1*, the gene encoding the largest known
13 potassium channel subunit, K_{Na}1.1, are associated with developmental and epileptic
14 encephalopathies accompanied by severe psychomotor and intellectual disabilities. Blocking
15 hyperexcitable K_{Na}1.1 channels with quinidine, a class I antiarrhythmic drug, has shown
16 variable success in patients due in part to dose-limiting off-target effects, poor blood-brain-
17 barrier penetration and low potency. In recent years, high-resolution cryo-EM structures of
18 the chicken K_{Na}1.1 channel in different activation states have been determined, and animal
19 models of the diseases have been generated. Alongside increasing information about the
20 functional effects of GOF pathogenic variants on K_{Na}1.1 channel behaviour and how they
21 lead to hyperexcitability, these tools will facilitate development of more effective treatment
22 strategies. Here, we review the range of *KCNT1* variants and their functional effects,
23 challenges posed by current treatment strategies, and recent advances in finding more
24 potent and selective therapeutic interventions for *KCNT1*-related epilepsies.

25 ***KCNT1* mutations are associated with treatment-resistant epilepsies**

26

27 To date, upwards of 50 distinct missense gain-of-function (GOF) pathogenic variants of
28 *KCNT1* have been associated with severe, refractory, developmental and epileptic
29 encephalopathies (DEE)[1]. *KCNT1* encodes the largest known potassium channel subunit,
30 $K_{Na}1.1$ (Slack, or previously Slo2.2 or $K_{Ca}4.1$), which forms a tetrameric Na^+ -activated K^+
31 channel. $K_{Na}1.1$ and the closely-related $K_{Na}1.2$ (encoded by *KCNT2*) subunits have distinct
32 expression patterns in the central nervous system (CNS) [2,3] but also co-localise in some
33 regions, and can form heteromeric co-assemblies [4,5]. In normal physiology, K_{Na} channels
34 are responsible for generation of the slow **afterhyperpolarisation** (AHP, see glossary)
35 following single action potentials [6,7] or bursts of action potential firing [8]. K_{Na} channels
36 have also been implicated as an important determinant of the resting membrane potential
37 and intrinsic excitability in a number of cell types in the CNS [9,10] and in arterial smooth
38 muscle [11].

39

40 Channelopathies of K^+ channels are found in a number of epilepsies, arising from both loss-
41 of-function (LOF) and GOF mutations [12]. *KCNT1* pathogenic variants appear to cause
42 significantly more severe clinical phenotypes, accompanied by intellectual and psychomotor
43 disabilities. The phenotypic spectrum is becoming increasingly broad, and inhibition of
44 overactive $K_{Na}1.1$ by class I antiarrhythmic quinidine as a treatment strategy has had limited
45 success [13-26]. However, there is accumulating information about the mechanisms
46 underlying the GOF effect of DEE-related *KCNT1* pathogenic variants. This, coupled with
47 high-resolution structures of the inactive and active states of $K_{Na}1.1$ generated by cryogenic

48 electron microscopy (cryo-EM) [27], has provided new opportunities for developing
49 therapeutic interventions.

50

51 **Range of *KCNT1* disorders**

52

53 Pathogenic *KCNT1* variants were first identified in two distinct epilepsies; epilepsy of infancy
54 with migrating focal seizures (EIMFS) and autosomal-dominant or sporadic sleep-related
55 hypermotor epilepsy ((AD)SHE) [28,29]. EIMFS is characterised by recurrent migrating,
56 polymorphous seizures, with a typical age of onset before 6 months, after which frequency
57 of seizures increases. The disorder is accompanied by other severe comorbidities such as
58 developmental disorders [30,31] and delayed motor function [32]. Following onset, patients
59 may lose all psychomotor skills previously developed [30]. *KCNT1* pathogenic variants have
60 been identified as the most prevalent variants in patients with EIMFS through whole exome
61 sequencing (WES) studies and result in large increases in $K_{Na}1.1$ current amplitude when
62 mutated channels are expressed *in vitro* [28,32]. Most EIMFS-associated *KCNT1* pathogenic
63 variants are *de novo*, though three separate cases of somatic mosaicism have been
64 identified [17,31,33]. The disorder is accompanied by other severe comorbidities such as
65 developmental and psychiatric disorders [30,31] and delayed motor function [32]. Following
66 onset, patients may lose all psychomotor skills previously developed [30].

67

68 (AD)SHE, clinically, is a less severe disorder, characterised by motor seizures occurring
69 during sleep, and a mean age of onset of 6 years old [29]. Seizures are, like EIMFS,
70 accompanied by cognitive disabilities. This separates them from (AD)SHE associated with
71 other genes, such as those encoding nicotinic acetylcholine receptor subunits. Furthermore,

72 (AD)SHE arising specifically from *KCNT1* is defined by more severe seizures and an earlier
73 age of onset than other forms of (AD)SHE [29].

74

75 *KCNT1* variants have been linked to other hyperexcitability disorders with psychomotor and
76 developmental defects, including Ohtahara syndrome [2,3], Lennox-Gastaut syndrome [26]
77 and Status Dystonicus [34]. There have also been reported cases of West syndrome,
78 leukoencephalopathies and Brugada syndrome [31]. Only one heterozygous LOF variant,
79 causing impaired $K_{Na}1.1$ trafficking, has thus far been reported in a patient that exhibited
80 severe generalised seizures and delayed myelination [35,36]. Cardiac effects have been
81 more recently reported, with pathogenic *KCNT1* variants linked to systemic-to-pulmonary
82 artery collateral-mediated heart disease, or 'collateralopathy' [37-39].

83

84 **Structure and function of $K_{Na}1.1$**

85

86 $K_{Na}1.1$ is a member of the SLO subfamily of K^+ channels [40], which exhibit unusually high
87 conductance, and are encoded by four genes in mammals [41]. $K_{Na}1.1$ subunits have
88 structural and functional similarities to other K^+ channels, such as $K_{Ca}1.1$ (BK_{Ca}) and the K_v
89 family of voltage-gated K^+ channels. $K_{Na}1.1$ subunits are, like K_v channels, composed of six
90 transmembrane helices and a loop between the S5 and S6 domains that forms the
91 selectivity filter [27,42]. The channel is weakly voltage-gated and mechanisms underlying its
92 voltage-sensitivity are unknown. Unlike K_v channels and other SLO subfamily subunits $K_{Ca}1.1$
93 and $K_{Ca}5.1$ (Slo3), $K_{Na}1.1$ does not possess a voltage-sensing domain (VSD) defined by an
94 excess of positively charged residues on its S4 domain [43]. Characteristic of all SLO
95 subfamily members, however, $K_{Na}1.1$ has a large intracellular C-terminal domain containing

96 two regulation of conductance of K⁺ (RCK) domains, and also multiple consensus sites for
97 PKC phosphorylation [27,42]. The C-terminal also contains a nicotinamide adenine
98 dinucleotide (NAD⁺) binding domain believed to be involved in potentiating channel activity
99 [44].

100

101 K_{Na}1.1 is primarily Na⁺-activated, despite its weak voltage-sensitivity; in the absence of
102 intracellular Na⁺, wildtype (WT) K_{Na}1.1 channels show almost no activity in whole-cell patch
103 clamp experiments [45]. Mutational studies have implicated the RCK domains in conferring
104 Na⁺ sensitivity of both K_{Na}1.1 and K_{Na}1.2 [46,47], though this is yet to be corroborated by
105 structural data. The exact mechanisms of channel gating have not been elucidated; there is
106 a narrowing of the intracellular pore vestibule by movement of the S6 helices to the
107 'closed', Na⁺-unbound state, yet there remains sufficient access to the selectivity filter by K⁺
108 ions [27]. This, and other recent functional studies of K_{Na}1.1 and closely related K_{Na}1.2, point
109 away from a canonical **S6 helix bundle-crossing** as the mechanism of activation gating
110 [48,49]. Rather, it is possible that the channel is gated either by a **hydrophobic gating**
111 mechanism or **selectivity filter gating** mechanism. This is similar to a number of other K⁺
112 channels that lack features of widely-accepted canonical mechanisms of voltage gating, for
113 example an S6 helix bundle-crossing and VSD [50-53].

114

115 Pathogenic GOF variants associated with DEEs are clustered in 'hotspots' in the channel
116 structure thought to be involved with gating; particularly around the RCK and NAD⁺ binding
117 domains. Pathogenic variants are also found in the pore-forming region on the S5 and S6
118 helices, and one pathogenic variant has been reported on the S3 helix (Figure 1), which
119 together with those in the intracellular domains may reflect disruption of a range of protein

120 regions that are critical for channel activation. It was earlier suggested that location of
121 mutation on the channel structure could be related to clinical phenotype [54], however
122 G288S located on the S5 helix, and R398Q located on RCK1, have since been reported to
123 cause both (AD)SHE and EIMFS [32,33]. Several mechanisms have been proposed for how
124 pathogenic variants may lead to GOF, such as changes in Na⁺ sensitivity [17,55,56] or
125 increased maximum probability of opening (P_o) [56]. Other studies have shown that
126 pathogenic variants increase cooperative gating between channels in the same patch
127 excised from *Xenopus* oocytes [32], or cause K_{Na}1.1 to be in a constitutively phosphorylated-
128 like state, as a result of altered interactions with binding proteins such as Phosphatase and
129 Actin Regulator 1 (Phactr1) [28,57,58]. Though pathogenic variants may alter channel
130 activity through different mechanisms, the overall effect is GOF characterised by an increase
131 in outward current amplitude, and a shift in the half-maximal activation voltage in the
132 hyperpolarising direction [14,55].

133

134 Missense *KCNT1* variants are almost always heterozygous, with patients carrying only one
135 mutated allele. Only one patient with Ohtahara syndrome has been reported as
136 homozygous, as a result of uniparental disomy [59]. Due to the severity of phenotypes
137 resulting from heterozygous *KCNT1* pathogenic variants, it is unlikely that homozygous
138 patients would survive. Most efforts to functionally characterise *KCNT1* pathogenic variants
139 involve expression of homomeric mutant channels. Recently, the implications of
140 heterozygous *KCNT1* pathogenic variants [14,55] or *KCNT2* pathogenic variants in co-
141 assembly with *KCNT1* [5] on channel function have been studied *in vitro* using co-
142 expression. These studies show heteromeric variant/WT channels behave with
143 characteristics ‘intermediate’ between WT and pathogenic variant homomeric channels. In

144 general, however, there is an absence of information concerning the functional and kinetic
145 effects of heterozygous pathogenic variants.

146

147 **Treatments and their rationale**

148

149 *KCNT1*-related epilepsies are intractable, with conventional therapies only temporarily
150 alleviating symptoms. Antiarrhythmic drugs quinidine and bepridil are efficacious at
151 inhibiting WT and pathogenic variant $K_{Na}1.1$ channels expressed in *Xenopus* oocytes and
152 mammalian cells [14,54,55,60,61]. A third antiarrhythmic drug, clofilium, has also been
153 found to inhibit WT channels *in vitro* [62]. These inhibitors are non-selective and inhibit
154 multiple ion channels, including cardiac cation channels [55,60,62], and only quinidine has
155 been trialled in patients.

156

157 Quinidine is a less potent inhibitor than bepridil; the drugs inhibit WT $K_{Na}1.1$ expressed in
158 mammalian cells with IC_{50} values in the order of 100 μ M and 1 μ M, respectively [55,60,61].
159 Both have been tested against several pathogenic *KCNT1* variants in whole-cell and single
160 channel patch clamp experiments [14,34,54,55,61]. When applied to two EIMFS-causing
161 variants, M516V and G288S, bepridil inhibited $K_{Na}1.1$ current more potently compared to
162 WT [55]. The same effect was reported when quinidine was tested against (AD)SHE-causing
163 variant Y796H [61]. This raises the possibility that the inhibitors exert an open-channel block
164 and the increase in channel activity with pathogenic $K_{Na}1.1$ variants may potentiate binding
165 by quinidine and bepridil [14,55].

166

167 Clinically, quinidine has led to variable results. One study reported only 20% of patients to
168 have more than 50% reduction in seizures, and another found 45% to have more than 25%
169 reduction [15,63]. Furthermore, *in vitro* efficacy does not fully translate to clinical efficacy;
170 clinical and *in vitro* effects of quinidine and other drugs are summarised in Table 1. For
171 example, despite promising inhibition of the variant Y796H expressed in *Xenopus* oocytes
172 and HEK293 cells [54,61], there was no improvement in (AD)SHE symptoms or
173 accompanying developmental symptoms [18]. On the other hand, whilst quinidine was not
174 as effective at reducing K629N K_{Na}1.1 currents as other variants, seizure frequency in a
175 patient carrying this EIMFS-causing variant was reduced by 80% [18,54]. In another EIMFS
176 patient, significant reduction of seizure frequency and developmental defects were
177 reported following quinidine therapy [13]. Since heteromeric channels comprising WT and
178 mutated subunits have properties intermediate of channels comprising WT or mutated
179 subunits alone [14,55], efficacy of K_{Na}1.1 inhibitors may also be influenced by this.

180

181 Quinidine has poor blood-brain-barrier (BBB) penetration and may not reach
182 therapeutically-significant concentration in the CNS [13,18]. A drug that crosses the BBB
183 effectively is desirable, due to the abundance of K_{Na}1.1 in the CNS [2,3]. No studies have
184 reported cerebrospinal fluid (CSF) concentration of quinidine in patients with *KCNT1*-related
185 DEEs. Previously, CSF levels of quinidine in humans were measured as between 4-37% of
186 unbound serum concentration [64], suggesting that even at therapeutic circulating
187 concentrations, lower levels reach the CNS. Varying serum quinidine concentrations have
188 been reported in a sample of 7 *KCNT1* patients, ranging 1.23-14.8 μ M [65]. The therapeutic
189 quinidine concentration range when used as an antiarrhythmic is 6-15 μ M, and toxic effects
190 occur at above 18.5 μ M [13]. Considering that quinidine inhibits K_{Na}1.1 *in vitro* with an IC₅₀

191 of 100 μM [55,60,61], it is unsurprising that clinical success is limited. Fitzgerald *et al* [15]
192 reported subtherapeutic levels of quinidine in more than half of the patients in their cohort.
193 Increasing the serum concentration to reach therapeutic levels may lead to off-target
194 effects, as was found in a randomised trial in 6 adult patients presenting with *KCNT1*-related
195 (AD)SHE (Australian Therapeutic Goods Administration Clinical Trial Registry, number
196 2015/0151) [19].

197

198 Combination therapy with hepatic cytochrome P450 enzyme-inducers, such as
199 phenobarbital and phenytoin, may hinder quinidine effectiveness by inducing its
200 metabolism and lowering serum concentrations by as much as 50%. This has been
201 evidenced in a patient with EIMFS resulting from two *KCNT1* variants, R356W and
202 P724_L728 dup, though the second is of unknown significance. Serum levels of quinidine
203 were undetectable prior to discontinuation of concurrent phenobarbital administration [21].
204 Similarly, two patients with EIMFS resulting from *KCNT1* pathogenic variants, G288S and
205 A934T, had decreased quinidine serum concentration resulting from combination therapy
206 with phenobarbital [24].

207

208 Bepridil, quinidine, and clofilium all present a problem with selectivity when used
209 therapeutically for epilepsies. Bepridil is primarily an L-type Ca^{2+} channel blocker, but also
210 inhibits fast inward Na^{+} current through voltage-gated Na^{+} channels in a similar manner to
211 lidocaine [66]. Quinidine inhibits human *ether-a-go-go*-related gene (hERG) K^{+} channels
212 expressed in HEK293 cells with an IC_{50} of 0.41 μM [67], which is several orders of magnitude
213 more potent than an IC_{50} in the order of 100 μM required to inhibit $\text{K}_{\text{Na}}1.1$ expressed in
214 mammalian cells [55,60,61]. Since all three inhibitors are potent inhibitors of hERG

215 channels, adverse cardiac effects may arise from their clinical use [13]. The hERG channel
216 current is responsible for termination of the cardiac action potential, and inhibition can
217 induce **Torsades de Pointes ventricular arrhythmia**, mimicking the type-2 long-QT (LQT)
218 syndrome phenotype [68]. Though some reports suggest increasing dosage and
219 consequently serum concentration in some patients may lead to LQT-like side effects,
220 Fitzgerald *et al* [15] found there to be no relationship between blood quinidine level and
221 propensity for prolonged **QTc interval**. This raises the possibility that a prolonged QTc
222 interval can present even with subthreshold concentrations of quinidine. There is an unmet
223 need for more potent and selective inhibitors of $K_{Na}1.1$ that suppress the effects of GOF
224 pathogenic variants.

225

226 **Mode of action of known inhibitors**

227

228 Whilst the mechanism of action of $K_{Na}1.1$ inhibitors was previously unknown, inhibition of
229 hERG channels by quinidine, bepridil and clofilium has been investigated in-depth. These
230 drugs block hERG by interacting with aromatic side chains of residues lining the inner pore
231 vestibule, which is largely hydrophobic, from the intracellular side. It is predicted that
232 inhibitors cross the plasma membrane and block the channel intracellularly [61]. A
233 phenylalanine residue located in the hERG channel pore, F656, was identified as a common
234 determinant of inhibition by the three inhibitors [69-72]. This led to the hypothesis that
235 quinidine and bepridil also bind to the inner pore vestibule of $K_{Na}1.1$. A combination of *in*
236 *silico* modelling of quinidine and bepridil binding within the pore (Figure 2), utilising
237 structures of the chicken $K_{Na}1.1$ channel and mutational analysis of the human $K_{Na}1.1$
238 channel, supported this [61]. Indeed, the residue identified as important for quinidine and

239 bepridil binding to K_{Na}1.1, F346, is the equivalent phenylalanine to that determining hERG
240 inhibition by quinidine, clofilium, and bepridil [69-72]. The same residue has also been
241 implicated in an EIMFS-causing *KCNT1* pathogenic variant, F346L and is thus far the only
242 variant found to be completely insensitive to inhibition by quinidine *in vitro*, when
243 expressed in *Xenopus* oocytes [17].

244

245 A number of small molecule inhibitors have been identified that inhibit the channel with
246 low- and sub-micromolar potencies. A combination of **structure-based virtual screening**
247 using a K_{Na}1.1 cryo-EM structure, and **ligand-based virtual screening** using bepridil as
248 reference, were used to identify inhibitors from a virtual library of 100,000 compounds. It
249 was proposed that the inhibitors had a similar mechanism of action to quinidine and
250 bepridil, blocking the channel via the intracellular vestibule (Figure 2). Furthermore, two of
251 the compounds had limited cytotoxicity and did not inhibit hERG channels in preliminary
252 toxicity screens. It is noteworthy that the two compounds identified that were structurally-
253 similar to bepridil almost completely inhibited hERG channels at 10 μM [61]. As well as
254 identifying potential pharmacophores, starting points for more potent inhibitors of K_{Na}1.1,
255 or tools to study the channel further, this work highlights the use of cryo-EM-derived
256 structures of membrane proteins for structure-based drug discovery. Though the structure
257 determined by Hite and MacKinnon [27] was that of chicken rather than human K_{Na}1.1, they
258 share 84% sequence homology. The success when testing the compounds against the
259 human K_{Na}1.1 channel demonstrates that proteins very close to the human structure can be
260 utilised in the absence of the desired structure.

261

262 More recently, a potent small molecule inhibitor, VU0606170, was identified using a high-
263 throughput **thallium flux screen**. This compound inhibited WT channels expressed in
264 HEK293 cells with an IC₅₀ of 1.84 μM, and EIMFS-causing pathogenic variant A934T with an
265 IC₅₀ of 1.16 μM. Further selectivity experiments found this compound to be inactive against
266 K_{Na}1.2, K_{Ca}1.1, GIRK1/2, K_v2.1, TREK1 potassium channels, and Ca_v3.2 and Na_v1.7. Though
267 the compound inhibited hERG channels to some degree, the potency was lower than
268 bepridil. Importantly, VU0606170 reduced the firing rate of hyperexcitable cultured cortical
269 rat neurons, providing evidence that selective K_{Na}1.1 inhibition may act to diminish
270 hyperexcitability [73]. Similarly, using another well-established high-throughput screen and
271 functional assays, Griffin *et al* [74] identified and characterised a small molecule inhibitor
272 with *in vivo* activity. Compound 31, an optimised derivative of a hit from a high-throughput
273 **rubidium flux screen**, reduced both seizure frequency and interictal spikes in a mouse
274 model of EIMFS-causing pathogenic variant P924L (mP905L). Compound 31 inhibited human
275 WT and mP905L channels *in vitro* with nanomolar and low micromolar potency respectively,
276 and was selective for K_{Na}1.1 channels over hERG, Na_v1.5, Ca_v1.2, I_{Ks}, K_{Ca}1.1, and K_{Na}1.2 [74].
277 It is surprising that both VU0606170 and Compound 31 are both selective for K_{Na}1.1 over
278 K_{Na}1.2 channels, considering their high sequence homology; sharing 78% sequence identity
279 and differing by only one residue in the pore vestibule. Whilst it is possible that these
280 molecules target different and less well-conserved domains of the channel, the reduced
281 potency of Compound 31 with F346L K_{Na}1.1 and the importance of trifluoromethyl groups
282 for potency, which in BC12 and BC14 were found to dock between the pore and S5 helices
283 [61] (Figure 2B), suggest that Compound 31 binds the channel pore in a similar manner.

284

285 **Potential new inhibitor modalities**

286

287 To date, the literature principally describe $K_{Na}1.1$ pore-blocking drugs, a mechanism linked
288 to non-selectivity due to similarity in structure and pore-lining residues between different K^+
289 channel subunits. Advances in structure-based drug design and information about the
290 underlying mechanisms of GOF pathogenic variants may give rise to alternative modalities
291 for therapeutics. Targeting other domains, such as those involved in ligand binding and
292 activation by either Na^+ or NADP, may provide alternative pharmacological opportunities.

293

294 Though many K^+ channels have conserved sequences, particularly around the selectivity
295 filter and pore-forming region, RCK domains on the C-terminus are one of the features
296 separating SLO channels from other eukaryotic K^+ channels [41]. Moreover, the RCK
297 domains of $K_{Na}1.1$ and $K_{Na}1.2$ deviate further from those of other members of the SLO
298 family due to the channel being activated by intracellular Na^+ . In place of the Ca^{2+} -bowl
299 possessed by $K_{Ca}1.1$ channels, which enables Ca^{2+} activation, the $\alpha Q'$ helix of $K_{Na}1.1$ is
300 extended across the assembly interface between RCK domains of adjacent subunits [42].

301 Though homomeric pathogenic variant $K_{Na}1.1$ channels are shown to have some activity in
302 the absence of intracellular Na^+ [55,56], the behaviour of heteromeric pathogenic variant
303 and WT channels in the absence of Na^+ has not been widely explored. It is possible that an
304 antagonist acting at the Na^+ - binding site of the channel could diminish the effects of GOF
305 pathogenic variants effectively, without residual activity in heteromeric channels.

306

307 Previous work using a combination of homology modelling, molecular simulations and
308 mutagenesis has highlighted a conserved aspartate residue as being important for Na^+ -
309 sensitivity of rat $K_{Na}1.1$ [46] and $K_{Na}1.2$ [47] channels. In $K_{Na}1.1$, rH823 and rD818 (hH844

310 and hD839) are part of a proposed Na⁺-binding motif, DXRXXH, which is responsible for Na⁺
311 sensitivity in G protein-coupled inwardly-rectifying K⁺ (GIRK) channels. Mutation of the
312 aspartate in this motif to neutral or positively-charged residues significantly reduced, but
313 did not abolish, Na⁺-sensitivity of the channel expressed in *Xenopus* oocytes [46]. This model
314 of Na⁺-activation does not align well with the since determined K_{Na}1.1 channel structure,
315 with the conserved loop containing this motif, including the equivalent aspartate side-chain
316 (cD812 in chicken K_{Na}1.1), remaining in the same conformation in the active and inactive
317 channel states [27]. Further information is required on the location of the residues involved
318 in Na⁺-binding to the RCK domains, and the mechanisms by which Na⁺-binding leads to
319 K_{Na}1.1 activation. Similarly, whether the NADP binding site can be targeted to prevent the
320 modulatory effects of NADP on Na⁺-activation [44] has yet to be explored.

321

322 K_{Na}1.1 has a number of modulatory cytoplasmic binding partners that could potentially be
323 targeted. For example, Fragile X Mental Retardation Protein (FMRP) increases P_o of K_{Na}1.1
324 [75], and TMEM16C directly interacts with K_{Na}1.1 subunits to increase Na⁺ sensitivity and
325 increase channel activity [76]. SCYL1 has also been found to increase P_o of K_{Na}1.1 when the
326 two proteins are co-expressed in *Xenopus* oocytes, and their overlapping expression
327 patterns in mouse brain regions suggests this binding protein may regulate K_{Na}1.1 activity in
328 neurons [77]. Preventing the physical or functional interaction with these proteins may
329 suppress hyperactive K_{Na}1.1 channel activity. Conversely, in HEK293T cells, co-expression
330 with Phactr1 suppresses rat K_{Na}1.1 current. It is hypothesised that this happens via protein
331 phosphatase 1-mediated (PP1) dephosphorylation of the channel at rS407 (hS426), the
332 critical PKC phosphorylation residue on the C-terminus of K_{Na}1.1 [58]. Suppression of K_{Na}1.1
333 by Phactr1 is disrupted by the introduction of two EIMFS-causing *KCNT1* pathogenic variants

334 [57]. The interaction between $K_{Na}1.1$ and Phactr1 may therefore also be a useful therapeutic
335 target.

336

337 $K_{Na}1.1$ channels are activated both by intracellular Na^+ and voltage, whilst lacking the
338 canonical VSD that is found in other voltage-gated K^+ channels [42]. Understanding the
339 interactions of domains that underly the WT $K_{Na}1.1$ gating mechanism would assist in
340 determining the effects of pathogenic variants on channel function, but also in finding new
341 treatment modalities. A negative allosteric modulator that uncouples the interaction
342 between Na^+ - binding and channel activation or affects the intrinsic closed-open transition
343 could act to suppress $K_{Na}1.1$, perhaps in a similar manner to modulators of $K_{Ca}1.1$ channels.
344 For example, paxilline allosterically modulates $K_{Ca}1.1$, by preferentially occupying the closed
345 state and decreasing the equilibrium constant L described in the Horrigan-Aldrich allosteric
346 model for channel gating, with the overall effect of suppressing current [78]. L describes the
347 intrinsic closed to open channel transition in the absence of Ca^{2+} , and no active VSD [79].

348

349 Though it is currently unclear how GOF *KCNT1* pathogenic variants may lead to
350 hyperexcitability, several mechanisms have been suggested. One such hypothesis is that
351 GOF of $K_{Na}1.1$ channels expressed in GABAergic inhibitory interneurons could increase
352 hyperpolarisation [80,81]. This would dampen their inhibitory effect on excitatory
353 interneurons, leading to increased excitation. This has been evidenced by
354 electrophysiological recordings from primary cortical neurons cultured from a mouse model
355 of (AD)SHE-causing mutation Y796H, which resulted in increased $K_{Na}1.1$ current at
356 subthreshold voltages in both non-fast and fast-spiking GABAergic neurons [81]. Another
357 possibility is that pathogenic variant $K_{Na}1.1$ channels activate rapidly in response to action

358 potentials, enabling more rapid recovery from action potentials. Voltage-gated Na⁺
359 channels, which are responsible for the upstroke of the action potential, may become
360 inactivated and re-primed at a faster rate, increasing the rate of high frequency firing and
361 leading to hyperexcitability. The latter was evidenced by a study of potentially immature
362 iPSC-derived neurons that harbour homozygous variant P924L K_{Na}1.1 through genome
363 editing [82]. This genotype, however, does not reflect the usual heterozygous nature of the
364 disorders and the function of homomeric mutant channels may differ from those co-
365 assembled with wild-type subunits.

366

367 Considering the potentially neuron-subtype-specific effects of *KCNT1* pathogenic variants, it
368 may be of use to target specific cell types therapeutically. Inhibiting subthreshold K_{Na}1.1
369 current in GABAergic inhibitory interneurons [81], particularly non-fast spiking neurons,
370 could reverse the effects of pathogenic variants on membrane excitability and action
371 potential generation.

372

373 **Concluding remarks and future perspectives**

374

375 Following the initial reports of pathogenic *KCNT1* variants [28,29], the broad spectrum of
376 disorders associated with K_{Na}1.1 has become apparent. Normal function of K_{Na}1.1 is
377 important not only for regulating neuronal excitability [6-10], but also for cardiac and
378 intellectual functions [11,37,38], evidenced by the wide range of phenotypes resulting from
379 pathogenic variants. Understanding the underlying mechanisms of GOF pathogenic variants,
380 particularly in heteromeric assemblies of mutant and WT subunits, will be key in developing
381 more effective and selective treatment strategies. Availability of high resolution cryo-EM

382 structures for the channel in different activation states [27,42], and animal models [83], will
383 aid this in future. As stated in the outstanding questions, determining how Na^+ acts to
384 activate $\text{K}_{\text{Na}1.1}$, and the sequence of events involved in gating the channel is important in
385 understanding how pathogenic variants exert their effects. This will enable other, more
386 selective, treatment modalities to be explored that suppress $\text{K}_{\text{Na}1.1}$ current and avoid off-
387 target cardiac effects.

388 References

389

390 1. Stenson, P.D. *et al.* (2020) The Human Gene Mutation Database (HGMD((R))): optimizing its
391 use in a clinical diagnostic or research setting. *Hum Genet* 139, 1197-1207. 10.1007/s00439-
392 020-02199-3

393 2. Rizzi, S. *et al.* (2016) Differential distribution of the sodium-activated potassium channels
394 slick and slack in mouse brain. *J Comp Neurol* 524, 2093-2116. 10.1002/cne.23934

395 3. Bhattacharjee, A. *et al.* (2002) Localization of the Slack potassium channel in the rat central
396 nervous system. *J Comp Neurol* 454, 241-254. 10.1002/cne.10439

397 4. Chen, H. *et al.* (2009) The N-terminal domain of Slack determines the formation and
398 trafficking of Slick/Slack heteromeric sodium-activated potassium channels. *J Neurosci* 29,
399 5654-5665. 10.1523/JNEUROSCI.5978-08.2009

400 5. Mao, X. *et al.* (2020) The Epilepsy of Infancy With Migrating Focal Seizures: Identification of
401 de novo Mutations of the KCNT2 Gene That Exert Inhibitory Effects on the Corresponding
402 Heteromeric KNa 1.1/KNa 1.2 Potassium Channel. *Front Cell Neurosci* 14, 1.
403 10.3389/fncel.2020.00001

404 6. Liu, X. and Stan Leung, L. (2004) Sodium-activated potassium conductance participates in the
405 depolarizing afterpotential following a single action potential in rat hippocampal CA1
406 pyramidal cells. *Brain Res* 1023, 185-192. 10.1016/j.brainres.2004.07.017

407 7. Franceschetti, S. *et al.* (2003) Na⁺-activated K⁺ current contributes to postexcitatory
408 hyperpolarization in neocortical intrinsically bursting neurons. *J Neurophysiol* 89, 2101-2111.
409 10.1152/jn.00695.2002

410 8. Yang, B. *et al.* (2007) Slack and Slick K(Na) channels regulate the accuracy of timing of
411 auditory neurons. *J Neurosci* 27, 2617-2627. 10.1523/JNEUROSCI.5308-06.2007

412 9. Lee, J.H. *et al.* (2019) The local translation of KNa in dendritic projections of auditory
413 neurons and the roles of KNa in the transition from hidden to overt hearing loss. *Aging*
414 (*Albany NY*) 11, 11541-11564. 10.18632/aging.102553

415 10. Reijntjes, D.O.J. *et al.* (2019) Sodium-activated potassium channels shape peripheral
416 auditory function and activity of the primary auditory neurons in mice. *Sci Rep* 9, 2573.
417 10.1038/s41598-019-39119-z

418 11. Li, P. *et al.* (2019) Sodium-activated potassium channels moderate excitability in vascular
419 smooth muscle. *J Physiol* 597, 5093-5108. 10.1113/JP278279

420 12. Villa, C. and Combi, R. (2016) Potassium Channels and Human Epileptic Phenotypes: An
421 Updated Overview. *Front Cell Neurosci* 10, 81. 10.3389/fncel.2016.00081

422 13. Bearden, D. *et al.* (2014) Targeted treatment of migrating partial seizures of infancy with
423 quinidine. *Ann Neurol* 76, 457-461. 10.1002/ana.24229

424 14. Dilena, R. *et al.* (2018) Early Treatment with Quinidine in 2 Patients with Epilepsy of Infancy
425 with Migrating Focal Seizures (EIMFS) Due to Gain-of-Function KCNT1 Mutations: Functional
426 Studies, Clinical Responses, and Critical Issues for Personalized Therapy. *Neurotherapeutics*
427 15, 1112-1126. 10.1007/s13311-018-0657-9

428 15. Fitzgerald, M.P. *et al.* (2019) Treatment Responsiveness in KCNT1-Related Epilepsy.
429 *Neurotherapeutics* 16, 848-857. 10.1007/s13311-019-00739-y

430 16. Madaan, P. *et al.* (2018) A quinidine non responsive novel KCNT1 mutation in an Indian
431 infant with epilepsy of infancy with migrating focal seizures. *Brain Dev* 40, 229-232.
432 10.1016/j.braindev.2017.09.008

433 17. McTague, A. *et al.* (2018) Clinical and molecular characterization of KCNT1-related severe
434 early-onset epilepsy. *Neurology* 90, e55-e66. 10.1212/WNL.0000000000004762

435 18. Mikati, M.A. *et al.* (2015) Quinidine in the treatment of KCNT1-positive epilepsies. *Ann*
436 *Neurol* 78, 995-999. 10.1002/ana.24520

- 437 19. Mullen, S.A. *et al.* (2018) Precision therapy for epilepsy due to KCNT1 mutations: A
438 randomized trial of oral quinidine. *Neurology* 90, e67-e72.
439 10.1212/WNL.0000000000004769
- 440 20. Numis, A.L. *et al.* (2018) Lack of response to quinidine in KCNT1-related neonatal epilepsy.
441 *Epilepsia* 59, 1889-1898. 10.1111/epi.14551
- 442 21. Passey, C.C. *et al.* (2019) Concurrent Quinidine and Phenobarbital in the Treatment of a
443 Patient with 2 KCNT1 Mutations. *Curr Ther Res Clin Exp* 90, 106-108.
444 10.1016/j.curtheres.2019.02.002
- 445 22. Patil, A.A. *et al.* (2019) Two South Indian Children with KCNT1-Related Malignant Migrating
446 Focal Seizures of Infancy - Clinical Characteristics and Outcome of Targeted Treatment with
447 Quinidine. *Ann Indian Acad Neurol* 22, 311-315. 10.4103/aian.AIAN_229_18
- 448 23. Takase, C. *et al.* (2020) KCNT1-positive epilepsy of infancy with migrating focal seizures
449 successfully treated with nonnarcotic antitussive drugs after treatment failure with
450 quinidine: A case report. *Brain Dev* 42, 607-611. 10.1016/j.braindev.2020.05.002
- 451 24. Yoshitomi, S. *et al.* (2019) Quinidine therapy and therapeutic drug monitoring in four
452 patients with KCNT1 mutations. *Epileptic Disord* 21, 48-54. 10.1684/epd.2019.1026
- 453 25. Alsaleem, M. *et al.* (2019) Infantile refractory seizures due to de novo KCNT 1 mutation. *BMJ*
454 *Case Rep* 12. 10.1136/bcr-2019-231178
- 455 26. Jia, Y. *et al.* (2019) Quinidine Therapy for Lennox-Gastaut Syndrome With KCNT1 Mutation. A
456 Case Report and Literature Review. *Front Neurol* 10, 64. 10.3389/fneur.2019.00064
- 457 27. Hite, R.K. and MacKinnon, R. (2017) Structural Titration of Slo2.2, a Na⁺-Dependent K⁺
458 Channel. *Cell* 168, 390-399.e311. 10.1016/j.cell.2016.12.030
- 459 28. Barcia, G. *et al.* (2012) De novo gain-of-function KCNT1 channel mutations cause malignant
460 migrating partial seizures of infancy. *Nat Genet* 44, 1255-1259. 10.1038/ng.2441
- 461 29. Heron, S.E. *et al.* (2012) Missense mutations in the sodium-gated potassium channel gene
462 KCNT1 cause severe autosomal dominant nocturnal frontal lobe epilepsy. *Nat Genet* 44,
463 1188-1190. 10.1038/ng.2440
- 464 30. Coppola, G. *et al.* (1995) Migrating partial seizures in infancy: a malignant disorder with
465 developmental arrest. *Epilepsia* 36, 1017-1024
- 466 31. Ohba, C. *et al.* (2015) De novo KCNT1 mutations in early-onset epileptic encephalopathy.
467 *Epilepsia* 56, e121-128. 10.1111/epi.13072
- 468 32. Kim, G.E. *et al.* (2014) Human slack potassium channel mutations increase positive
469 cooperativity between individual channels. *Cell Rep* 9, 1661-1672.
470 10.1016/j.celrep.2014.11.015
- 471 33. Møller, R.S. *et al.* (2015) Mutations in KCNT1 cause a spectrum of focal epilepsies. *Epilepsia*
472 56, e114-120. 10.1111/epi.13071
- 473 34. Gertler, T.S. *et al.* (2019) Functional consequences of a KCNT1 variant associated with status
474 dystonicus and early-onset infantile encephalopathy. *Ann Clin Transl Neurol* 6, 1606-1615.
475 10.1002/acn3.50847
- 476 35. Evely, K.M. *et al.* (2017) The Phe932Ile mutation in KCNT1 channels associated with severe
477 epilepsy, delayed myelination and leukoencephalopathy produces a loss-of-function channel
478 phenotype. *Neuroscience* 351, 65-70. 10.1016/j.neuroscience.2017.03.035
- 479 36. Vanderver, A. *et al.* (2014) Identification of a novel de novo p.Phe932Ile KCNT1 mutation in a
480 patient with leukoencephalopathy and severe epilepsy. *Pediatr Neurol* 50, 112-114.
481 10.1016/j.pediatrneurol.2013.06.024
- 482 37. Kawasaki, Y. *et al.* (2017) Three Cases of KCNT1 Mutations: Malignant Migrating Partial
483 Seizures in Infancy with Massive Systemic to Pulmonary Collateral Arteries. *J Pediatr* 191,
484 270-274. 10.1016/j.jpeds.2017.08.057
- 485 38. Kohli, U. *et al.* (2020) Cardiac phenotypic spectrum of KCNT1 mutations. *Cardiol Young*, 1-5.
486 10.1017/S1047951120002735

- 487 39. Ikeda, A. *et al.* (2021) Recurrent pulmonary hemorrhage in juvenile patients with KCNT1
488 mutation. *Pediatr Int* 63, 352-354. 10.1111/ped.14427
- 489 40. Yuan, A. *et al.* (2003) The sodium-activated potassium channel is encoded by a member of
490 the Slo gene family. *Neuron* 37, 765-773. 10.1016/s0896-6273(03)00096-5
- 491 41. Salkoff, L. *et al.* (2006) High-conductance potassium channels of the SLO family. *Nat Rev*
492 *Neurosci* 7, 921-931. 10.1038/nrn1992
- 493 42. Hite, R.K. *et al.* (2015) Cryo-electron microscopy structure of the Slo2.2 Na(+)-activated K(+)
494 channel. *Nature* 527, 198-203. 10.1038/nature14958
- 495 43. Kaczmarek, L.K. (2013) Slack, Slick and Sodium-Activated Potassium Channels. *ISRN Neurosci*
496 2013. 10.1155/2013/354262
- 497 44. Tamsett, T.J. *et al.* (2009) NAD+ activates KNa channels in dorsal root ganglion neurons. *J*
498 *Neurosci* 29, 5127-5134. 10.1523/JNEUROSCI.0859-09.2009
- 499 45. Bhattacharjee, A. and Kaczmarek, L.K. (2005) For K+ channels, Na+ is the new Ca2+. *Trends*
500 *Neurosci* 28, 422-428. 10.1016/j.tins.2005.06.003
- 501 46. Zhang, Z. *et al.* (2010) The RCK2 domain uses a coordination site present in Kir channels to
502 confer sodium sensitivity to Slo2.2 channels. *J Neurosci* 30, 7554-7562.
503 10.1523/JNEUROSCI.0525-10.2010
- 504 47. Thomson, S.J. *et al.* (2015) Identification of the Intracellular Na+ Sensor in Slo2.1 Potassium
505 Channels. *J Biol Chem* 290, 14528-14535. 10.1074/jbc.M115.653089
- 506 48. Giese, M.H. *et al.* (2017) Molecular mechanisms of Slo2 K+ channel closure. *J Physiol* 595,
507 2321-2336. 10.1113/JP273225
- 508 49. Garg, P. *et al.* (2013) Structural basis of ion permeation gating in Slo2.1 K+ channels. *J Gen*
509 *Physiol* 142, 523-542. 10.1085/jgp.201311064
- 510 50. Kopec, W. *et al.* (2019) Molecular mechanism of a potassium channel gating through
511 activation gate-selectivity filter coupling. *Nat Commun* 10, 5366. 10.1038/s41467-019-
512 13227-w
- 513 51. Nematian-Ardestani, E. *et al.* (2020) Selectivity filter instability dominates the low intrinsic
514 activity of the TWIK-1 K2P K. *J Biol Chem* 295, 610-618. 10.1074/jbc.RA119.010612
- 515 52. Schewe, M. *et al.* (2016) A Non-canonical Voltage-Sensing Mechanism Controls Gating in K2P
516 K(+) Channels. *Cell* 164, 937-949. 10.1016/j.cell.2016.02.002
- 517 53. Lolicato, M. *et al.* (2017) K2P2.1(TREK-1):activator complexes reveal a cryptic selectivity filter
518 binding site. *Nature* 547, 364-368. 10.1038/nature22988
- 519 54. Milligan, C.J. *et al.* (2014) KCNT1 gain of function in 2 epilepsy phenotypes is reversed by
520 quinidine. *Ann Neurol* 75, 581-590. 10.1002/ana.24128
- 521 55. Rizzo, F. *et al.* (2016) Characterization of two de novo KCNT1 mutations in children with
522 malignant migrating partial seizures in infancy. *Mol Cell Neurosci* 72, 54-63.
523 10.1016/j.mcn.2016.01.004
- 524 56. Tang, Q.Y. *et al.* (2016) Epilepsy-Related Slack Channel Mutants Lead to Channel Over-
525 Activity by Two Different Mechanisms. *Cell Rep* 14, 129-139. 10.1016/j.celrep.2015.12.019
- 526 57. Fleming, M.R. *et al.* (2016) Stimulation of Slack K(+) Channels Alters Mass at the Plasma
527 Membrane by Triggering Dissociation of a Phosphatase-Regulatory Complex. *Cell Rep* 16,
528 2281-2288. 10.1016/j.celrep.2016.07.024
- 529 58. Ali, S.R. *et al.* (2020) Phactr1 regulates Slack (KCNT1) channels via protein phosphatase 1
530 (PP1). *FASEB J* 34, 1591-1601. 10.1096/fj.201902366R
- 531 59. Martin, H.C. *et al.* (2014) Clinical whole-genome sequencing in severe early-onset epilepsy
532 reveals new genes and improves molecular diagnosis. *Hum Mol Genet* 23, 3200-3211.
533 10.1093/hmg/ddu030
- 534 60. Yang, B. *et al.* (2006) Pharmacological activation and inhibition of Slack (Slo2.2) channels.
535 *Neuropharmacology* 51, 896-906. 10.1016/j.neuropharm.2006.06.003
- 536 61. Cole, B.A. *et al.* (2020) Structure-Based Identification and Characterization of Inhibitors of
537 the Epilepsy-Associated K. *iScience* 23, 101100. 10.1016/j.isci.2020.101100

- 538 62. de Los Angeles Tejada, M. *et al.* (2012) Clofilium inhibits Slick and Slack potassium channels.
539 *Biologics* 6, 465-470. 10.2147/BTT.S33827
- 540 63. Borlot, F. *et al.* (2020) KCNT1-related epilepsy: An international multicenter cohort of 27
541 pediatric cases. *Epilepsia* 61, 679-692. 10.1111/epi.16480
- 542 64. Ochs, H.R. *et al.* (1980) Entry of quinidine into cerebrospinal fluid. *Am Heart J* 100, 341-346.
543 10.1016/0002-8703(80)90148-9
- 544 65. Abdelnour, E. *et al.* (2018) Does age affect response to quinidine in patients with KCNT1
545 mutations? Report of three new cases and review of the literature. *Seizure* 55, 1-3.
546 10.1016/j.seizure.2017.11.017
- 547 66. Li, Y. *et al.* (1999) Bepridil blunts the shortening of action potential duration caused by
548 metabolic inhibition via blockade of ATP-sensitive K(+) channels and Na(+)-activated K(+)
549 channels. *J Pharmacol Exp Ther* 291, 562-568
- 550 67. Paul, A.A. *et al.* (2002) Inhibition of the current of heterologously expressed HERG potassium
551 channels by flecainide and comparison with quinidine, propafenone and lignocaine. *Br J*
552 *Pharmacol* 136, 717-729. 10.1038/sj.bjp.0704784
- 553 68. Finlayson, K. *et al.* (2004) Acquired QT interval prolongation and HERG: implications for drug
554 discovery and development. *Eur J Pharmacol* 500, 129-142. 10.1016/j.ejphar.2004.07.019
- 555 69. Macdonald, L.C. *et al.* (2018) Probing the molecular basis of hERG drug block with unnatural
556 amino acids. *Sci Rep* 8, 289. 10.1038/s41598-017-18448-x
- 557 70. Kamiya, K. *et al.* (2006) Molecular determinants of HERG channel block. *Mol Pharmacol* 69,
558 1709-1716. 10.1124/mol.105.020990
- 559 71. Knape, K. *et al.* (2011) In silico analysis of conformational changes induced by mutation of
560 aromatic binding residues: consequences for drug binding in the hERG K⁺ channel. *PLoS One*
561 6, e28778. 10.1371/journal.pone.0028778
- 562 72. Perry, M. *et al.* (2004) Structural determinants of HERG channel block by clofilium and
563 ibutilide. *Mol Pharmacol* 66, 240-249. 10.1124/mol.104.000117
- 564 73. Spitznagel, B.D. *et al.* (2020) VU0606170, a Selective Slack Channels Inhibitor, Decreases
565 Calcium Oscillations in Cultured Cortical Neurons. *ACS Chem Neurosci* 11, 3658-3671.
566 10.1021/acscchemneuro.0c00583
- 567 74. Griffin, A.M. *et al.* (2021) Discovery of the First Orally Available, Selective KNa1.1 Inhibitor: In
568 Vitro and In Vivo Activity of an Oxadiazole Series. *ACS Medicinal Chemistry Letters* 12, 593-
569 602. 10.1021/acsmchemlett.0c00675
- 570 75. Zhang, Y. *et al.* (2012) Regulation of neuronal excitability by interaction of fragile X mental
571 retardation protein with slack potassium channels. *J Neurosci* 32, 15318-15327.
572 10.1523/JNEUROSCI.2162-12.2012
- 573 76. Huang, F. *et al.* (2013) TMEM16C facilitates Na(+)-activated K⁺ currents in rat sensory
574 neurons and regulates pain processing. *Nat Neurosci* 16, 1284-1290. 10.1038/nn.3468
- 575 77. Niu, L.G. *et al.* (2020) Slo2 potassium channel function depends on RNA editing-regulated
576 expression of a SCYL1 protein. *Elife* 9. 10.7554/eLife.53986
- 577 78. Zhou, Y. and Lingle, C.J. (2014) Paxilline inhibits BK channels by an almost exclusively closed-
578 channel block mechanism. *J Gen Physiol* 144, 415-440. 10.1085/jgp.201411259
- 579 79. Horrigan, F.T. and Aldrich, R.W. (2002) Coupling between voltage sensor activation, Ca²⁺
580 binding and channel opening in large conductance (BK) potassium channels. *J Gen Physiol*
581 120, 267-305. 10.1085/jgp.20028605
- 582 80. Kuchenbuch, M. *et al.* (2021) In silico model reveals the key role of GABA in KCNT1-epilepsy
583 in infancy with migrating focal seizures. *Epilepsia* 62, 683-697. 10.1111/epi.16834
- 584 81. Shore, A.N. *et al.* (2020) Reduced GABAergic Neuron Excitability, Altered Synaptic
585 Connectivity, and Seizures in a KCNT1 Gain-of-Function Mouse Model of Childhood Epilepsy.
586 *Cell Rep* 33, 108303. 10.1016/j.celrep.2020.108303

- 587 82. Quraishi, I.H. *et al.* (2019) An Epilepsy-Associated KCNT1 Mutation Enhances Excitability of
588 Human iPSC-Derived Neurons by Increasing Slack KNa Currents. *J Neurosci* 39, 7438-7449.
589 10.1523/JNEUROSCI.1628-18.2019
- 590 83. Quraishi, I.H. *et al.* (2020) Impaired motor skill learning and altered seizure susceptibility in
591 mice with loss or gain of function of the Kcnt1 gene encoding Slack (K. *Sci Rep* 10, 3213.
592 10.1038/s41598-020-60028-z
- 593 84. Datta, A.N. *et al.* (2019) Two Patients With KCNT1-Related Epilepsy Responding to
594 Phenobarbital and Potassium Bromide. *J Child Neurol* 34, 728-734.
595 10.1177/0883073819854853
- 596 85. Cataldi, M. *et al.* (2019) Migrating focal seizures in Autosomal Dominant Sleep-related
597 Hypermotor Epilepsy with KCNT1 mutation. *Seizure* 67, 57-60.
598 10.1016/j.seizure.2019.02.019
599
600

601 Glossary

602

603 **Afterhyperpolarisation:** Repolarisation of the membrane potential following an action
604 potential or burst of action potentials. The membrane potential falls lower than resting
605 membrane potential, and this is usually facilitated by K⁺ channel activation.

606

607 **Hydrophobic gating:** In K⁺ channels gated by a hydrophobic gate, water transitions between
608 liquid and vapour states within the pore as it interacts with hydrophobic pore-lining
609 residues. In the vapour state, the pore cavity becomes 'de-wetted' or collapsed, and this
610 acts as a barrier to ion permeation. De-wetting is dependent on pore diameter.

611

612 **Ligand-based virtual screening:** Computer-aided drug screening technique that identifies
613 structurally similar compounds to a known ligand from a chemical library. These structurally
614 similar compounds can later be docked into the protein of interest and ranked based on
615 predicted binding affinity.

616

617 **QTc interval:** On an ECG, the QTc interval is defined as the time interval between the start
618 of the Q wave, and end of the T wave. This represents the onset of depolarisation, and end
619 of repolarisation of the cardiac action potential.

620

621 **Rubidium flux screen:** A high-throughput technique with the capability to screen large
622 libraries of compounds for K⁺ channel modulation, exploiting the ability of Rb⁺ to permeate
623 the channels. Cells can be pre-incubated with ⁸⁶RbCl and the degree of efflux during the
624 assay can be determined by liquid scintillation. Alternately, cells can be loaded with cold
625 RbCl and efflux determined by atomic absorption.

626

627 **S6 helix bundle-crossing:** The canonical mechanism of K⁺ channel gating. The cytoplasmic
628 end of S6 helices of K⁺ channel subunits converge at the bottom of the pore-forming region,
629 forming a 'bundle crossing'. Ion conduction is physically occluded by the S6 helix
630 bundle crossing and widening enables ion conduction.

631

632 **Selectivity filter gating:** A recently identified mechanism of K⁺ channel gating. The selectivity
633 filter widens as a result of allosteric coupling with the activation gate, facilitated by pore-
634 lining transmembrane helices, to enable ion conduction.

635

636 **Structure-based virtual screening:** Computer-aided drug screening approach involving
637 docking compounds from a chemical library into a protein structure. Intermolecular
638 interactions can be predicted, and chemicals are ranked based on predicted binding
639 affinities.

640

641 **Thallium flux screen:** Fluorescence-based assay that utilises the permeability of Tl⁺ through
642 K⁺ channels, to detect modulators of K⁺ channels heterologously expressed in mammalian
643 cells. A high-throughput technique with the capability to screen large libraries of
644 compounds.

645

646 **Torsades de Pointes ventricular arrhythmia:** Associated with prolongation of the QTc
647 interval, this acquired or inherited arrhythmia is characterised by 'twisting' of the QRS
648 segment of an ECG. Torsades de Pointes can sometimes lead to ventricular fibrillation and
649 cardiac arrest.

650

651 Figure Legends

652

653 **Figure 1 Structure of the K_{Na}1.1 potassium channel and location of mutated residues.** Cryo-
654 EM structure of the chicken K_{Na}1.1 channel in the active conformation (PDB: 5U70 [27]).
655 One subunit of the tetramer is coloured yellow with the residues coloured red indicating
656 those that are altered in the equivalent position in human K_{Na}1.1 by *KCNT1* gain-of-
657 function pathogenic variants. Figure prepared in UCSF Chimera.

658

659 **Figure 2 Predicted interactions between K_{Na}1.1 and inhibiting compounds.** A Structure of
660 the pore domain of the tetrameric chicken K_{Na}1.1 channel [27] comprising the S5, P-loop,
661 and S6 segments. The yellow dashed box indicates the region depicted in the figures in
662 panel B. B Docking poses of quinidine, bepridil, BC13, and BC14 from the study by Cole *et*
663 *al.* [61] in the K_{Na}1.1 channel pore. Compounds occupy the pore and interact with
664 residues in the S6 segment and also those immediately below the selectivity filter. Potency
665 of each of these inhibitors was reduced by mutation of a phenylalanine in S6 (shown at the
666 bottom of each figure) to serine [61]. Figure prepared in UCSF Chimera.

667

Table 1: Pathogenic variants in *KCNT1* that have been studied *in vitro* or clinically with inhibitors, their location on the channel structure, and the associated clinical phenotype.

| Pathogenic variant | CDS change | Location | Associated disorder | Pharmacological modulation <i>in vitro</i> | Clinical response to therapies | References |
|---------------------------------|-----------------------------------|---------------------|---------------------|--|--|------------------|
| R209C | c.625C>T | S3 domain | Lennox-Gastaut | N/A | Clinically significant response to quinidine | [26] |
| A259D | c.776C>A | S4-5 linker | EIMFS | Quinidine significantly decreased current amplitude (300 μ M) | No clinical response to quinidine | [20] |
| Q270E | c.808C>G | S5 domain | EIMFS | N/A | No clinical response to quinidine No clinical response to quinidine or ketogenic diet | [16,63] |
| V271F | c.811G>T | S5 domain | EIMFS | Quinidine significantly decreased current amplitude (300 μ M) | N/A | [17] |
| L274I | c.820C>A | S5 domain | EIMFS | Quinidine significantly decreased current amplitude (300 μ M) | No clinical response to quinidine Patient showed minimal response to ketogenic diet and no response to cannabidiol | [17,63] |
| G288S | c.862G>A | S5 domain | (AD)SHE EIMFS | Bepiridil significantly more potent compared to WT IC₅₀ for bepridil: 0.15±0.05 μM No significant difference between inhibition of WT and mutant by quinidine IC₅₀ for quinidine: 67±19 μM Inhibited by test compound 31 IC₅₀: 221 nM | Some patients have responded to quinidine, others have not No clinical response to quinidine, seizures worsened. Phenobarbital showed slight efficacy but discontinued due to drowsiness. Three patients responded to quinidine, two out of the three had a marked response to ketogenic diet. The third had a marked response to cannabidiol. | [15,24,55,63,74] |
| F346L | c.1038C>G | S6 domain | EIMFS | Completely insensitive to quinidine (300 μ M) in <i>Xenopus</i> oocytes Inhibited by test compound 31 IC₅₀: 1.77 μM | N/A | [17,74] |
| R356W/ P724_L728 dup | c.1066C>T c.2170_2184dup 15 | Bottom of S6 domain | EIMFS | N/A | Minor relief with quinidine. Interaction with phenobarbital, resulting in prolonged QTc interval. | [21] |
| R398Q | c. 1193G>A | RCK1 domain | (AD)SHE EIMFS | Quinidine significantly decreased current amplitude (300 μ M) | No clinical response to quinidine | [54,63] |

| Pathogenic variant | CDS change | Location | Associated disorder | Pharmacological modulation <i>in vitro</i> | Clinical response to therapies | References |
|--------------------|------------|-------------|---------------------------------|---|---|------------------|
| R428Q | c.1283G>A | RCK1 domain | EIMFS | Quinidine significantly decreased current amplitude (300µM) | <p>Patient responded to phenobarbital and potassium bromide (later died of sudden cardiac arrest). Quinidine exacerbated seizures and was discontinued.</p> <hr/> <p>Patient responded to quinidine in combination with other antiepileptic medications and ketogenic diet</p> <hr/> <p>>50% reduction in seizure frequency with quinidine, experienced ventricular tachycardia. Seizures unresponsive to phenobarbital, KBr, clonazepam, clobazam, levetiracetam.</p> <hr/> <p>Patient showed marked response to ketogenic diet, some response to cannabidiol and no response to quinidine.</p> | [17,24,25,63,84] |
| L437F | c.1309C>T | RCK1 domain | Epilepsy with status distonicus | IC₅₀ for quinidine: 66 µM | N/A | [34] |
| R474C | c.1420C>T | RCK1 domain | Focal epilepsy | N/A | 23% reduction in seizure frequency with quinidine; not considered successful. No clinical response to conventional epilepsy therapeutics, methyl prednisolone pulse therapy, and ketogenic diet. | [24] |
| R474G | c.1420C>G | RCK1 domain | Multifocal seizures | N/A | Clinically significant response to phenobarbital | [84] |
| R474H | c.1421G>A | RCK1 domain | EIMFS | N/A | <p>No clinical response to quinidine</p> <hr/> <p>One patient responded to ketogenic diet, another showed no response to quinidine</p> <hr/> <p>Patient responded to tipepidine and dextromethorphan</p> | [15,23,63] |
| F502V | c.1504T>G | RCK1 domain | EIMFS | Quinidine significantly decreased current amplitude (300 µM) | Clinically significant response to quinidine | [17] |
| M516V | c.1546A>G | RCK1 domain | EIMFS | <p>Bepidil significantly more potent compared to WT</p> <p>IC₅₀ for bepidil: 0.3±0.1 µM</p> <p>No significant difference between inhibition of WT and mutant by quinidine</p> <p>IC₅₀ for quinidine: 46±12 µM</p> | N/A | [55] |
| K629N | c.1887G>C | RCK2 domain | EIMFS | Quinidine (300 µM) less effective than when used for Y796H, R428Q and WT | Clinically significant response to quinidine; 80% decrease in seizure frequency | [18,54] |

| Pathogenic variant | CDS change | Location | Associated disorder | Pharmacological modulation <i>in vitro</i> | Clinical response to therapies | References |
|--------------------|------------|--|---------------------|--|--|------------------|
| Y796H | c.2386T>C | NAD ⁺ binding domain | (AD)SHE | IC₅₀ for quinidine: 38±12.89 μM IC₅₀ for bepridil: 12.8±2.48 μM Inhibited by test compounds BC5,6,7,12,13 and 14 with IC₅₀ values ranging from 3.61-17.45 μM | No clinical response to quinidine | [18,61] |
| E893K | c.2677G>A | NAD ⁺ binding domain | EIMFS | More sensitive to quinidine than WT in CHO cells IC₅₀ for quinidine: 9.6±2.5 μM | Clinically significant response to quinidine; 90% reduction in seizures | [14] |
| M896K | c.2687T>A | NAD ⁺ binding domain | EIMFS | Quinidine significantly decreased current amplitude (300 μM) | Severe pulmonary vasculopathy resulting from clinical use of quinidine | [17] |
| M896I | c.2688 G>C | NAD ⁺ binding domain | SHE | Quinidine significantly decreased current amplitude (300 μM) | N/A | [54] |
| P924L | c.2771C>T | C-terminus (next to NAD ⁺ binding domain) | EIMFS | Quinidine significantly decreased current amplitude (300 μM) Mouse orthologue inhibited by test compound 31 IC₅₀: 1.012 μM | N/A | [54,74] |
| R928C | c.2782C>T | C-terminus (next to NAD ⁺ binding domain) | (AD)SHE | Quinidine significantly decreased current amplitude (300 μM) | No clinical response to quinidine | [19,54] |
| A934T | c.2800G>A | C-terminus (next to NAD ⁺ binding domain) | EIMFS | Quinidine significantly decreased current amplitude (300 μM) Inhibited by test compound VU0606170. IC₅₀: 1.16 μM | Clinically significant response to quinidine Seizure frequency initially decreased, but later increased with quinidine therapy. In combination with phenobarbital and KBr, phenobarbital hindered increase in quinidine serum levels One patient showed a marked response to both ketogenic diet and cannabidiol. Another responded to quinidine and low glycemic index diet. A third patient showed no clinical response to quinidine or ketogenic diet | [22,24,54,63,73] |
| R950Q | c.2849G>A | C-terminus | EIMFS | More sensitive to quinidine than WT in CHO cells IC₅₀ for quinidine: 24±5.7 μM | No clinical response to quinidine. Significant reduction in seizure frequency in another patient with quinidine therapy. One patient showed some response to cannabidiol therapy, another showed a marked response to quinidine and some response to low glycemic index diet | [14,22,63] |
| L962P | c.2885T>C | C-terminus | EIMFS | N/A | Some clinical response to ketogenic diet | [63] |

| Pathogenic variant | CDS change | Location | Associated disorder | Pharmacological modulation <i>in vitro</i> | Clinical response to therapies | References |
|---------------------------|---------------------------------|-------------------|--|--|--|-------------------|
| A966T | c.2896G > A | C-terminus | Combination of (AD)SHE and EIMFS phenotype | N/A | Complete and persistent response to phenobarbital in patient | [85] |
| R1114W/ del 550 | c.3340 C>T c.1649-1651delAGC | End of C-terminus | EIMFS | Quinidine significantly decreased current amplitude of R1114W variant (300 μM) but not del 550 variant | No clinical response to quinidine | [20] |

Highlights

Gain-of-function pathogenic variants of *KCNT1*, the gene encoding Na⁺-activated K⁺ channel K_{Na}1.1, underlie a broad spectrum of severe and refractory developmental and epileptic encephalopathies accompanied by intellectual disabilities.

KCNT1 variants likely cause hyperexcitability by impairing GABAergic neuron excitability. Inhibition of mutant K_{Na}1.1 channels is the current strategy to suppress hyperexcitability.

Known inhibitors block the inner pore vestibule of K_{Na}1.1, similar to how they inhibit cardiac hERG channels. Potent inhibition of hERG is one of the limiting factors for their use, along with low potency.

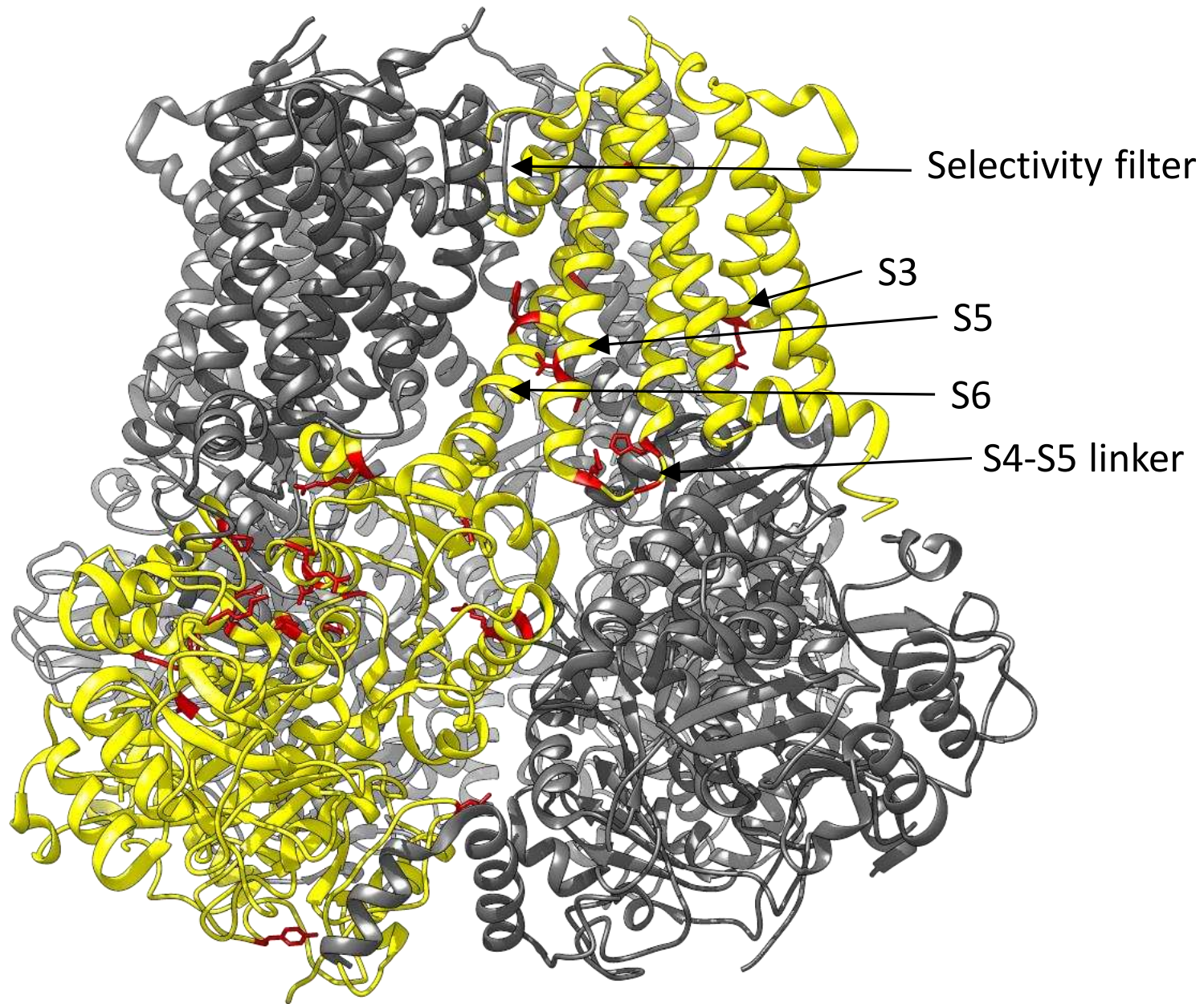
Potent small-molecule inhibitors of the channel have been identified, using both high-throughput screening and *in silico* methods. These inhibitors show promise both in terms of improved selectivity for K_{Na}1.1 and efficacy for suppressing hyperexcitable neurons.

Outstanding questions

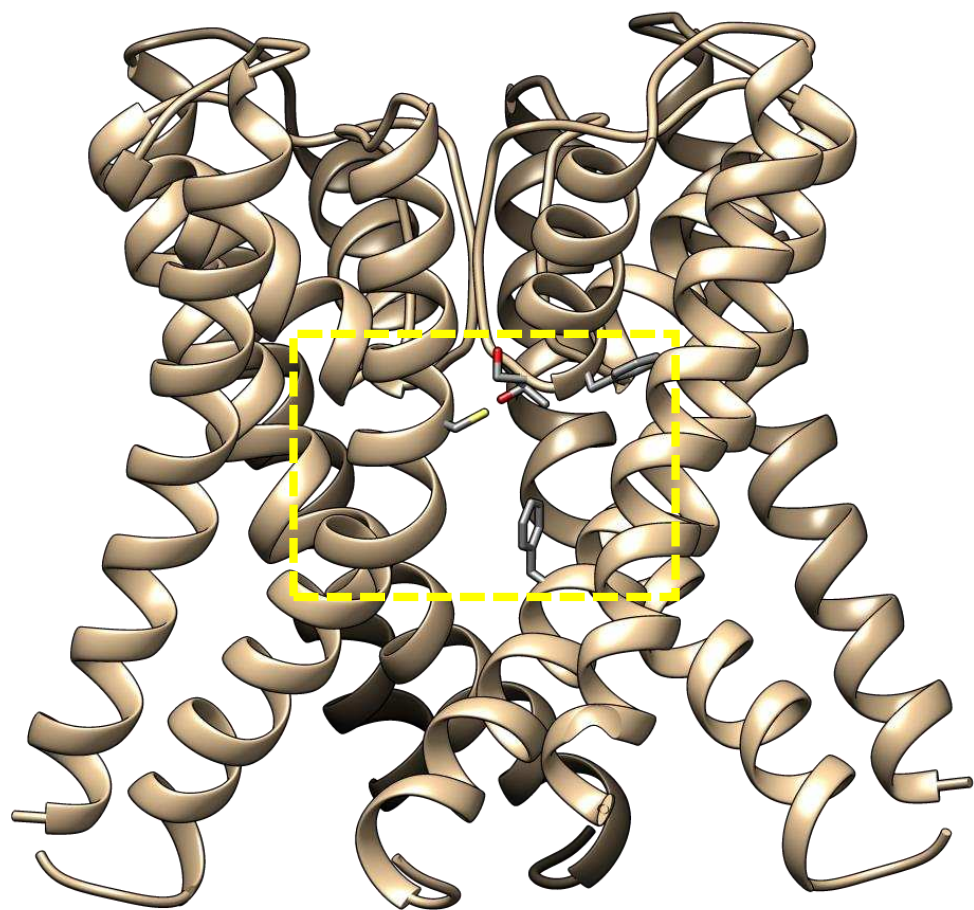
- How is $K_{Na}1.1$ activated by intracellular Na^+ ?
- How do Na^+ sensing and voltage interact to gate $K_{Na}1.1$, and how is this affected by epilepsy-causing mutants?
- How does heteromeric assembly of mutant and WT $K_{Na}1.1$ subunits affect inhibition and gating of the channel?

Transmembrane

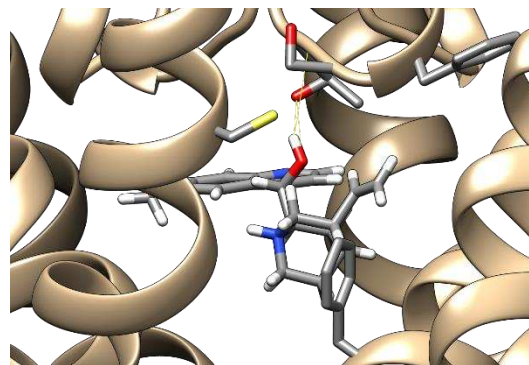
Intracellular



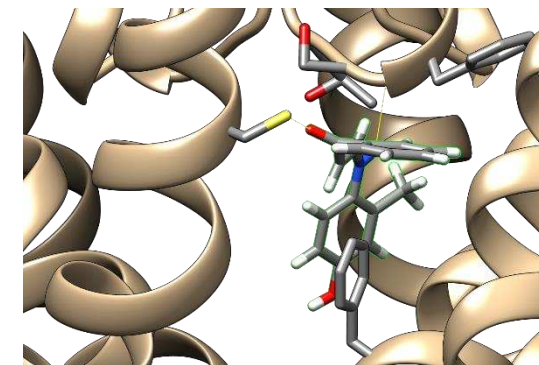
A



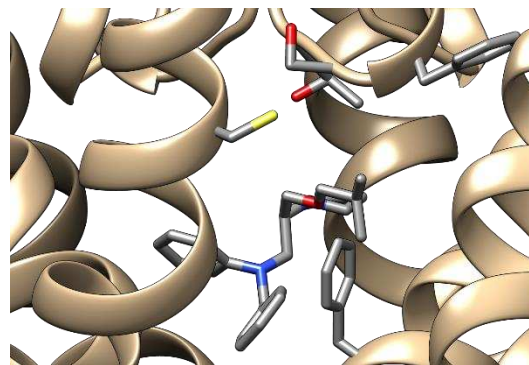
B



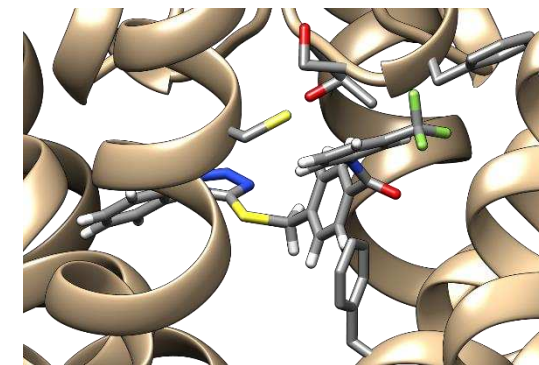
quinidine



BC13



bepridil



BC14